Exploring the relationship between MOPITT and in situ observations of CO based on a large-scale feature sampled during TRACE-P

J. H. Crawford,[1] C. L. Heald,[2] H. E. Fuelberg,[3] D. M. Morse,[3] G. W. Sachse,[1] L. K. Emmons,[4] J. C. Gille,[4] D. P. Edwards,[4] G. Chen,[1] J. R. Olson,[1] V. S. Connors,[1] C. Kittaka,[1] and A. J. Hamlin[1,5]

[1]Atmospheric Sciences, NASA Langley Research Center, Hampton, VA
[2]Department of Earth and Planetary Sciences, Harvard University, Cambridge, MA
[3]Department of Meteorology, Florida State University, Tallahassee
[4]National Center for Atmospheric Research, Boulder, CO
[5]Michigan Technological University, Houghton

1   **Abstract.**   During TRACE-P, there were several opportunities to perform in situ sampling

2   coincident with overpasses of the MOPITT instrument onboard the EOS Terra satellite.   This

3   sampling consisted of in situ vertical profiles of CO by NASA's DC-8 aircraft intended to provide

4   data useful for validating MOPITT observations of CO column.   One particular profile conducted

5   over the central North Pacific revealed a layer of pollution characterized by CO mixing ratios more

6   than double background values.   Sampling of the surrounding region by both the NASA DC-8 and

7   P-3B aircraft showed this layer to have a considerable geographic extent, at least 25 degrees

8   longitude (~2500 km) and 4 degrees latitude (~400 km).   Using back-trajectory analysis, this

9   polluted layer is followed back in time and compared with four consecutive MOPITT overpasses.

10   MOPITT observations during these four overpasses agree well with the location of the layer as

11   inferred by the trajectories; however, the detected CO column amount increases backward in time

12   by just over 20 percent.   Further analysis shows that the majority of this change in detected column

13   abundance is consistent with two factors: 1) changes in the thickness of the polluted layer over time

14   and 2) changes in retrieved column abundance due to the altitude of the layer.   An unexpected

15   finding was the difference in variability for MOPITT observations between day and night. Daytime

16   variability was approximately double that observed for nighttime data. The results of this analysis

17   and their implications for improving satellite validation strategies are discussed.

1. Introduction

Observations of tropospheric composition are essential to improving our understanding of chemical cycles and their role in the short-term and long-term evolution of the troposphere. Overcoming the paucity of observations continues to be one of the primary challenges to answering key questions about the sources and fates of various chemical species. Historically, in situ observations from aircraft have been the primary means of gathering observations of atmospheric composition throughout the free troposphere and over remote oceanic regions. Measurements from sondes and balloon-borne platforms have also played an important role but have been more limited in the number of species observed. More recently, satellite observations are becoming a significant source of information concerning tropospheric composition [Singh and Jacob, 2000]. The promise of much better temporal and spatial resolution from space-based observations, albeit for only a few species, promises to greatly complement airborne observations which are temporally and spatially limited but offer a wealth of detail on composition by the simultaneous measurement of many constituents. It is important then to fully explore the complementary relationship between airborne and satellite observations as opportunities arise.

Spaced-based observations have played a key role in previous airborne missions, most notably NASA's TRACE-A (Transport and Atmospheric Chemistry near the Equator - Atlantic) campaign [*Fishman et al.*, 1996] which deployed to the tropical South Atlantic. The impetus for TRACE-A was the satellite-derived observation of a region of enhanced tropospheric ozone off the west coast of southern Africa during austral spring [*Fishman et al.*, 1990]. NASA's more recent TRACE-P (Transport and Chemical Evolution over the Pacific) campaign [*Jacob et al.*, 2003] presented the first opportunity for a NASA airborne mission focused on tropospheric chemistry to interact directly with a space-based platform. During TRACE-P, NASA's DC-8 aircraft measured in situ vertical

1

1   profiles of CO coincident with overpasses of MOPITT (Measurements of Pollution in The

2   Troposphere). MOPITT represents one of the first satellite instruments to provide routine

3   measurements of a tropospheric constituent (carbon monoxide, CO) from space. The intent of these

4   in situ CO profiles was to provide data for validation. In addition to in situ measurements in support

5   of MOPITT, global model calculations also have been used to bridge the gap between the aircraft

6   and MOPITT observations of CO from the TRACE-P time period with encouraging results [*Heald*

7   *et al.*, this issue].

8   There were seven occasions during TRACE-P when the NASA DC-8 performed validation

9   profiles beneath the MOPITT instrument. Details of these under-flights and the resulting data

10 comparisons are discussed by *Jacob et al.* [2003]. One profile conducted during a transit flight over

11 the central Pacific revealed an enhanced layer of pollution with CO mixing ratios more than double

12 background values. Further sampling during transit revealed that this layer possessed a surprising

13 level of homogeneity for CO and other trace species over an extent of approximately 25 degrees of

14 longitude (~2500 km) across the central North Pacific.

15 The following work attempts to extend the linkage between MOPITT and the in situ data beyond

16 the validation profile coinciding with the MOPITT overpass. Using back-trajectory analysis, the

17 polluted layer is examined as a large regional feature, both at the time of aircraft sampling and back

18 in time through previous satellite overpasses. This offers the opportunity to assess the relationship

19 between in situ data and MOPITT observations in a way that is more comprehensive, albeit less

20 rigorous, than that provided by the single point comparison of the validation profile.

2. Instrument Descriptions

2.1. In situ

In situ measurements of CO were performed using a folded-path, differential absorption, tunable diode laser spectrometer [*Sachse et al.*, 1987; *Vay et al.*, 1998]. Two versions of the instrument were deployed during TRACE-P; one on NASA's DC-8 aircraft and the other on NASA's P-3B aircraft. Measurements were obtained at a frequency of 1 hz and a precision of 1 ppbv or 1%. Calibrations were performed on 10 minute intervals with measurement accuracy closely tied to the primary calibration standards obtained from the NOAA Climate Monitoring and Diagnostics Laboratory. Intercomparison of the two instruments during close proximity flight of the two aircraft revealed that the instruments agreed within the stated uncertainties [*Eisele et al.*, 2003].

2.2. MOPITT

The MOPITT instrument was launched aboard NASA's EOS Terra satellite in December, 1999. This downward viewing instrument uses IR gas correlation radiometry to monitor tropospheric CO and CH_4 [Drummond and Mand, 1996] and is capable of making observations during both day and night (CO only). MOPITT's polar sun-synchronous orbit has an equator crossing time of 10:45 local time. The horizontal resolution of MOPITT observations is 22 km x 22 km with cross-track scanning covering a swath 640 km wide. This cross-track scanning allows for near global coverage in 3 days. CO concentrations are reported for the total column amount and for 7 vertical levels (surface, 850, 700, 500, 350, 250, and 150 hPa).

The MOPITT observations used in this analysis are the version 3 retrievals for total CO column [http://www.eos.ucar.edu/mopitt]. Details on the MOPITT retrieval algorithm can be found in *Deeter et al.* [2003]. Data for individual levels were not used since they offer limited additional information. Specifically, an analysis of MOPITT data for the TRACE-P time period by *Heald et*

1   *al.* [this issue] determined that there are typically fewer than two pieces of independent information

2   per MOPITT pixel over the North Pacific. This is related in part to MOPITT's sensitivity which is

3   minimized at the surface and maximized in the middle troposphere [*Deeter et al.*, 2003]. In order

4   to compare in situ profiles with MOPITT, the vertical resolution and sensitivity of the MOPITT

5   retrievals must be taken into account using the appropriate averaging kernel and a priori profile. In-

6   depth discussion of comparing in situ data to MOPITT and the contribution of TRACE-P data to the

7   broader MOPITT validation effort can be found in *Emmons et al.* [submitted to J. Geophys. Res.,

8   2003].

9

10   **3. Observations of CO for 27 February, 2001**

11   On 27 February 2001 both the NASA DC-8 and P-3B aircraft departed from Kona, Hawaii (19N,

12   156W) on transit flights across the central, North Pacific. The destinations for the DC-8 and P-3B

13   were Guam (13N, 145E) and Wake Island (19N, 167E), respectively. During these flights, both

14   aircraft performed extensive atmospheric profiling. In the case of the DC-8, one of the profiles was

15   conducted coincident with an overpass of the MOPITT satellite with the intent of providing data

16   useful for validation. In-situ CO data for that profile are presented in Figure 1a. The comparison

17   with MOPITT is also shown. As noted above, this comparison required averaging the in situ data

18   to the 7-level vertical resolution of MOPITT followed by application of the appropriate MOPITT

19   averaging kernel (the "processed" data). As shown in Figure 1a, the agreement between MOPITT

20   and the processed in situ data is quite good.

21   Figure 1b shows the vertical distribution of CO observed from both aircraft between longitudes

22   of 170E and 165W. These data encompass 10 soundings; 6 by the P-3B from near-surface to ~ 470

23   hPa (6 km) and 4 by the DC-8 from near-surface to ~225 hPa (11 km). The in situ soundings reveal

4

1   a persistent polluted layer located between approximately 600 and 800 hPa. The sharp transition in

2   CO at 800 hPa coincides with the tradewind inversion capping the top of the marine boundary layer.

3   The temperature contrast across the inversion was of 4-6 degrees C (not shown). There was also a

4   sharp gradient in water vapor, with order of magnitude changes observed between the dry polluted

5   layer (~500-1000 ppmv H_2O) and the wetter conditions only 20-25 hPa below the bottom of the

6   layer.

7   Figure 1c shows the geographic distribution of the samples taken within this polluted layer and

8   their proximity to the MOPITT overpass. Observations covered 25 degrees longitudinally (~2500

9   km) and about 4 degrees latitudinally (~400 km). Trajectories from the aircraft sampling locations

10   indicate that this layer originated from the Asian Pacific Rim between 30-40N latitude

11   approximately 4 days earlier. Following rapid transport to the central Pacific, the polluted airmass

12   became somewhat stagnant, spending the next 3 days subsiding and drifting southward over the

13   central North Pacific. Given the size of the airmass and its stagnant behavior, taking a closer look

14   at this feature through multiple MOPITT overpasses would be informative. The ability to track such

15   a feature through satellite observations would make an important contribution to understanding the

16   fate of Asian emissions and their impact on the global atmosphere.

17

18   **4. Approach**

19   While the aircraft data indicate a polluted layer of broad geographic coverage, its full extent

20   cannot be deduced from in situ observations alone. However, an estimate of its extent has been

21   derived for this study based on an analysis of back-trajectories. These trajectories provide a bridge

22   between the in situ observations and the MOPITT overpasses.

23   A cluster of back-trajectories was calculated between 10-25N and 162E-165W with 1x1 degree

5

1   resolution. This area was deliberately chosen to be large enough to ensure that all trajectories

2   associated with the polluted layer could be isolated. Back-trajectories were initialized at 00 UT, 28

3   February 2001 which was the center of the temporal window of the aircraft observations in Figure

4   1b. Back-trajectories were initialized from the center of the polluted layer (700 hPa) as well as near

5   the upper and lower boundaries of the layer (615 hPa and 800 hPa). The trajectories initialized at

6   700 hPa are the primary trajectories used to trace the movement of the polluted layer. As will be

7   discussed in section 5.2, trajectories at 615 hPa and 800 hPa are used to estimate changes in the

8   thickness of the polluted layer.

9   The trajectory calculations utilized the global gridded meteorological analyses prepared by the

10   European Centre for Medium-Range Weather Forecasts (ECMWF) [*Bengtsson*, 1985; *Hollingsworth*

11   *et al.*, 1986; *ECMWF*, 1995]. The ECMWF analyses were available four times daily (0000, 0600,

12   1200, and 1800 UTC) at 60 vertical levels with a T319 spherical harmonic triangular truncation,

13   interpolated to a 1x1 degree latitude-longitude horizontal grid. Back trajectories were calculated

14   using a kinematic model employing u, v, and w wind components from the ECMWF analyses.

15   Additional details about the trajectory model are given in *Fuelberg et al.* [1996, 1999, 2000].

16   Limitations of trajectories have been discussed by *Stohl* [1998], *Fuelberg et al.* [2000], and *Maloney*

17   *et al.* [2001]. For these particular trajectories, their uncertainty most likely is dominated by their

18   location in a remote, data-sparse region. The meteorological setting suggests that errors due to

19   subscale processes (e.g., deep convection) are minimal given the slow subsidence of air during the

20   recent history of the trajectories.

21   The overall trajectory cluster was filtered to isolate the subset exhibiting a common origin from

22   the Asian Pacific Rim. Figure 2 shows the behavior and extent of the polluted layer as inferred from

23   the filtered subset of trajectories. These trajectories clearly show the stagnation and subsidence of

6

1 the polluted airmass over the 3 days prior to sampling by the aircraft. They also suggest that the

2 polluted layer had a latitudinal extent well beyond that which could be determined from the aircraft

3 data alone. The longitudinal extent agrees well with the observations, with the exception of the far

4 western end of the aircraft sampling. Trajectories from this area take a somewhat different pathway

5 back to the Asian Pacific Rim than the filtered data. This may represent some uncertainty in the

6 exact placement of the polluted airmass as diagnosed by the trajectories. While individual trajectory

7 errors can be quite large, the overall uncertainty in tracking the airmass is mitigated by its size and

8 the number of trajectories exhibiting similar behavior. Fortunately, overlap between the filtered

9 trajectories and the MOPITT overpasses do not occur near the western edge of the feature.

10 In the following section, the overlap between back-trajectories and several MOPITT overpasses

11 is examined. Overlap between MOPITT and the trajectories was defined by identifying those

12 MOPITT pixels (22x22 km) and trajectories (1x1 deg) within a proximity of +/- 0.5 deg in both

13 latitude and longitude.

14

15 **5. Results and Analysis.**

16 Figure 3 offers a qualitative assessment of the correspondence between the MOPITT CO column

17 observations and the polluted layer as determined through back-trajectories. In all cases there is a

18 general enhancement in MOPITT CO column for the region of overlap with trajectories. Lower

19 values of CO column are observed both north and south of the overlap in each case. This behavior

20 gives confidence that there is a signal in the MOPITT data that is associated with the polluted layer

21 observed by the aircraft and that this signal can be tracked back in time for several satellite

22 overpasses. An interesting feature of the correspondence is that CO column amounts appear to

23 intensify for earlier overpasses. This intensification is quantified by the statistics in Table 1. The

7

1 difference between average MOPITT CO column at the time of the TRACE-P flights on 27 February

2 $(2.27 \times 10^{18}$ molec cm$^{-2})$ and 36 hours earlier on 26 February $(2.75 \times 10^{18}$ molec cm$^{-2})$ represents an

3 increase of 21 percent. Understanding this change in CO column associated with the polluted layer

4 requires an examination of several factors. These factors include the impacts of dilution and

5 chemistry, changes in the thickness of the polluted layer, and the sensitivity of the MOPITT retrieval

6 to the vertical distribution of CO.

7 **5.1. Chemistry and Dilution**

8 Chemistry and dilution are expected to have little influence on the observed changes in CO

9 column. The average CO lifetime within the enhanced layer based on box model calculations is

10 estimated to be 45 days (diurnal average OH $= 1.2 \times 10^6$ molec cm^{-3}). Given that lifetime, the loss

11 of CO over the 36 hours between overpasses is only 3%. Calculated CO formation due to the

12 oxidation of methane and other hydrocarbons is expected to increase CO by about 0.5%, leading to

13 a net loss of only 2.5%. Calculations indicate a somewhat faster loss for CO below the polluted

14 layer and a slower loss above; however, these differences offset each other such that the 2.5%

15 estimate for the change in CO within the polluted layer is also a reasonable estimate of the expected

16 change in total CO column. Long-term observations of CO by *Novelli et al.* [1998] suggest that

17 typical changes in background CO for the Northern Hemisphere are even smaller (<1% per day).

18 Although contributions from dilution cannot be entirely eliminated from consideration, several

19 observations suggest that dilution played a minor role in the observed changes in CO column over

20 the 36 hours shown in Figure 3. First, CO values in the polluted layer are equivalent to median

21 values observed in the marine boundary layer along the Asian Pacific Rim during TRACE-P and

22 exceed the 75th percentile for Pacific Rim observations at 2-4 km. Thus, the CO concentrations in

23 the layer remain comparable to values observed near the source. Given the meteorological setting

1   of subsidence under the high pressure region, there is little expectation of strong vertical mixing.

2   This is supported by the rather steep vertical gradient in CO between the plume and background CO

3   both above and below the polluted layer. Horizontal mixing also would be limited by the sheer

4   extent of the feature since the mixing would be limited to the edges of the polluted airmass. Finally,

5   a polluted layer observed in the upper troposphere during the DC-8 flight of the previous day was

6   found to have a common origin with the polluted layer analyzed here [*Heald et al.*, this issue].

7   Heald et al. note that trajectory analysis shows that the polluted airmass separated into two branches;

8   one subsided over the central Pacific, and the other continued to be transported eastward in the upper

9   troposphere over the Pacific. A comparison of these two branches by Heald et al. revealed similar

10   chemical signatures and equivalent enhancements in both CO and total NO_y, suggesting that these

11   branches had experienced minimal dilution over this short time period.

12   **5.2. Thickness of the Polluted Layer**

13   The trajectories in Figure 2 exhibit gradual descent during the 3 days prior to sampling by the

14   NASA aircraft. As noted earlier, this sinking motion was arrested by the presence of the tradewind

15   inversion which marks the lower boundary of the polluted layer. As the descending airmass

16   encountered this inversion, it likely experienced some degree of flattening and horizontal spreading

17   under continued high pressure. This produced the rather broad but vertically compact layer of

18   pollution that was observed. Thus, earlier in time, the polluted layer likely had a greater thickness

19   which would lead to greater total CO column, albeit over a smaller area.

20   Results for trajectories initiated at 615 hPa and 800 hPa support the idea that the difference in

21   detected CO column is at least partially explained by changes in the thickness of the polluted layer

22   between overpasses. Based on the pressure difference between these two sets of trajectories, the

23   statistics in Table 1 show the layer to be approximately 1.5 times thicker (282 vs 190 hPa) on 26

1 February (0938 UT) than when it was ultimately sampled by the TRACE-P aircraft 36 hours later

2 on 27 February (2231 UT). An independent estimate of layer thickness using only the trajectories

3 initiated at 700 hPa can be derived based on the number of trajectories versus MOPITT pixels in the

4 overlap. For the 27 February (2231 UT) overpass, 98 trajectories overlapped with 1091 pixels (11.1

5 pixels/trajectory), and for the 26 February (0938 UT) overpass, 84 trajectories overlapped with 622

6 pixels (7.4 pixels/trajectory). The reduction in pixel/trajectory density indicates a 1/3 reduction in

7 geographic (horizontal) coverage which would be consistent with a 50 percent increase in layer

8 thickness.

9   Changes to total CO column amount due to a change in the thickness of the polluted layer

10 depends on the contribution of the pollution enhancement to the total column amount. Based on the

11 in situ data, the pollution enhancement contributes roughly 20 percent to the column total. However,

12 a more appropriate assessment comes from applying the MOPITT averaging kernel to the in situ

13 profile as it was sampled and with the pollution enhancement removed. This results in CO column

14 amounts of 2.36×10^{18} and 2.00×10^{18} molec cm^{-2}; thus the pollution enhancement contributes 18

15 percent to the column amount as detected by MOPITT. Based on the 18 percent contribution to total

16 CO column and the 50 percent increase in layer thickness, changes in layer thickness would be

17 sufficient to explain a 9 percent ($\pm$3 percent given the uncertainty in the thickness) change in average

18 CO column detected by MOPITT.

19 **5.3. Sensitivity of the MOPITT Retrieval to the Vertical Distribution of CO**

20   In addition to changes in layer thickness, changes in the altitude of the polluted layer are also

21 expected to affect the CO column amount detected by MOPITT, based on the vertical sensitivity of

22 the averaging kernel. This issue has been explored by applying the MOPITT averaging kernel to

23 the in situ profile of Figure 1a with the polluted layer displaced upward and downward by 100 hPa

10

1   increments. The results of this sensitivity analysis are shown by the crosses in Figure 4. Note that

2   the actual in situ CO column amount is unchanged; thus, the changes in MOPITT retrieved CO

3   column do not represent a change in the real column amount but only a change in the detected

4   column based on the applying the averaging kernel to different vertical distributions of CO. The

5   total range of sensitivity falls between 2.09 and 2.74×10^{18} molec cm^{-2}.

6   Average MOPITT CO column and vertical displacement for the overlap between MOPITT and

7   the trajectories initiated at 700 hPa are also shown in Figure 4 (also see numbers in Table 1). While

8   the trajectory-derived change in altitude over the 36 hour period between overpasses is just over 100

9   hPa , this change occurs at pressures where MOPITT is quite sensitive to vertical displacement of

10   the layer.   Based on the retrieval sensitivity (see crosses in Figure 4), changes in the altitude of the

11   polluted layer contributes about 7 percent ($\pm$ 3 percent given the uncertainty in average pressure

12   level) to the retrieved change in average CO column observed over the 36 hour period.

13   The effect of changes in the altitude of the polluted layer are further examined in Figure 5. Here

14   all individual MOPITT observations within the overlap are shown along with the estimated vertical

15   displacement based on the nearest trajectory. One initial observation is that the range of observed

16   MOPITT values is much greater under daylight conditions (Note: Since observations were made

17   near the international dateline, data for 2231 UT, 27 February and 2148 UT, 26 February represent

18   daylight conditions). This greater variability is also reflected in the standard deviations for CO

19   column reported in Table 1. These numbers indicate that daylight data exhibit approximately twice

20   the variability of data collected at night.

21   There is a strong relationship between vertical displacement and CO column for the nighttime

22   data on 26 February (0938 UT). The lack of a relationship for data from previous overpasses should

23   be acknowledged; however, this may be due to the greater variability for the daytime data and the

1   smaller range of vertical displacement in prior overpasses. The data for 26 February (0938 UT)

2   exhibit displacements of as much as 200 hPa and show a strong correlation between CO column and

3   displacement (R^2=0.63). This correlation between CO column and displacement provides

4   confidence that the sensitivity of MOPITT observations to changes in the vertical distribution of CO

5   are consistent with expectations. As discussed in the previous section, the wholesale shift in the data

6   toward larger CO columns is related to the increased thickness of the polluted layer on 26 February

7   (0938 UT).

8   The differences between daylight and nighttime MOPITT data seen in Figure 5 need to be

9   understood. Since retrievals are sensitive to surface temperature, day/night differences in MOPITT

10   observations over land are expected [*Deeter et al.*, 2002, 2003]. Observations over open ocean,

11   however, are expected to experience minimal day/night influence. The additional daytime

12   variability is not accounted for by the reported error in MOPITT column CO. Average reported

13   errors are actually less for the daytime data (6-7%) than for the nighttime data (9-10%) shown in

14   Figure 5.

15   One possible source of the day/night difference in variability that can be investigated is the

16   difference in cloud detection for daylight and dark conditions. The presence of clouds in MOPITT

17   pixels is determined using both MOPITT temperature retrievals and the MODIS (Moderate

18   Resolution Imaging Spectroradiometer) cloud mask product (details are available at

19   http://www.eos.ucar.edu/mopitt/data/index.html; Retrieval Information). An important benefit of

20   incorporating the MODIS cloud mask is the ability to identify low cloud. Retrievals over low cloud

21   are possible since MOPITT is insensitive to the lowest portion of the atmosphere. MOPITT's flag

22   for cloud description allows for 16 different possibilities, but only 4 occur for the data examined

23   here:

1   1 - clear, only MOPITT thermal used

2   2 - MOPITT and MODIS cloud mask agree on clear

3   3 - MODIS cloud mask only clear (when MOPITT determines cloudy)

4   4 - MOPITT overriding MODIS cloud mask over low clouds (MODIS test flags used).

5   Table 2 gives MOPITT CO column statistics for the various cloud flags under daylight and dark

6   conditions. While there is a difference in the distribution of cloud flags between daylight and dark,

7   these cloud flags do not appear to have a significant influence on average statistics for MOPITT CO

8   column. Under dark conditions, the dominant condition is a cloud flag of 4 (>70% of data). For

9   daylight conditions, the data are more evenly split between cloud flags of 2 and 4. The similarity

10   in CO statistics under daylight conditions for cloud flags 2 and 4 show that the MOPITT strategy

11   of using MODIS to discriminate for low cloud is effective.

12   While the difference in day/night variability remains unresolved, a cursory look at MOPITT data

13   for other days over the central, North Pacific shows that the disparity between day/night variability

14   exists, but may be smaller on average than what is suggested by this one case study. Nevertheless,

15   the issue warrants further study.

16

17   **6. Discussion and Implications**

18   The most encouraging result of this analysis is that the behavior of the MOPITT data is

19   consistent with expectations. From the statistics in Table 1, the average CO column for 26 February

20   (0938 UT) is increased over that of 27 February (2231 UT) by a ratio of 1.21. The majority of this

21   difference is consistent with two effects: the change in layer thickness (9 percent) and the change

22   in MOPITT sensitivity to the altitude of the layer (7 percent). The product of these two differences

23   yields a ratio of 1.17 which would account for 80 percent of the observed change in average CO

13

1   column. Adding the estimated impact of chemistry (2.5 percent) brings the estimate to within 10%

2   of the observed change. While not conclusive, this level of closure lends confidence to the idea that

3   the major factors contributing to the observed change in CO column have been identified.

4   The results of this analysis are beneficial in several ways: 1) they contribute to a better

5   understanding of the sources of variability in satellite observations, 2) they provide the basis for

6   exploring alternative strategies for validation and in situ sampling in support of satellite

7   observations, and 3) they demonstrate the link between satellite observations and the detailed

8   process studies pursued by research aircraft.

9   **6.1. Sources of Variability**

10   Of the seven validation profiles flown during TRACE-P, only four were in skies clear enough

11   to yield a comparison with MOPITT. The variation in MOPITT retrieved CO column for those four

12   attempts was only 16%. The variation across the four overpasses analyzed here was 21% and could

13   have been greater (~30 percent based on Figure 4) if the polluted layer had been traceable further

14   back in time. The fact that this change was due to multiple factors (both real and artificial)

15   highlights the importance of taking opportunities to integrate in situ and satellite data to better

16   understand the possible sources of variation in satellite observations. The difference in day/night

17   data also represents an important unexplained source of variability.

18   **6.2. Validation and Sampling in Support of Satellites**

19   While rigorous validation requires in situ profiles coincident with observations from satellite,

20   this analysis suggests that additional insight can be gained from a broader sampling of the

21   surrounding region as well. It also suggests that validation profiles could benefit from a targeted

22   approach aimed at pursuing large-scale features. For instance, additional back-trajectories from the

23   central North Pacific during the TRACE-P period (February-March, 2001) indicate that emissions

1   from the Asian Pacific Rim are transported to the central North Pacific in a manner similar to that

2   shown in this analysis roughly once every 10 days. This transport as well as cross-Pacific transport

3   of Asian emissions can be reasonably predicted by global models [*Heald et al.*, this issue] and could

4   be used as a guide to the best opportunities for taking in situ measurements in coordination with

5   satellites. Improving the ability to observe the behavior and frequency of individual large scale

6   perturbations as they transport emissions from source regions to remote regions is important for

7   understanding the incorporation of source emissions into the global atmosphere.

8   The day/night differences in variability (see Table 1 and Figure 5) suggest that validation of

9   MOPITT CO measurements may be best accomplished at night. Since validations are essentially

10   a point comparison between an in situ profile and the satellite, daytime validation would seem to

11   require a greater number of profiles to achieve the same accuracy as nighttime validation for

12   assessing the agreement between in situ and satellite observations. This suggestion should be

13   limited to marine environments given that sensitivity over land is significantly reduced near the

14   surface at night over day [*Deeter et al.*, 2003]. Thus, daytime validation over land is expected to

15   be more rigorous in that there will typically be higher information content in the retrievals and a

16   lower a priori fraction.

17   This analysis would be much more definitive if in situ data had been available for each of the

18   four consecutive overpasses, but one must also ask whether such a goal is realistic. Certainly it

19   would be worthwhile to test the ability of forward-trajectories and global (or regional) model

20   predictions to identify large-scale features and dictate the optimal times for conducting validation

21   profiles. The primary complicating factor would be waiting to see whether the feature and the

22   satellite would intersect for consecutive overpasses, the probability of which would largely depend

23   on the size of the feature.

6.3. Linking Satellite Observations and Detailed Process Studies

The polluted layer analyzed here was characterized by enhanced mixing ratios for many constituents in addition to CO. Of particular importance, ozone mixing ratios in excess of 80 ppbv were encountered in the layer, representing values well above those observed in air closer to the Asian Pacific Rim during TRACE-P. Understanding the photochemical evolution of this air mass as it relates to ozone production, the interconversion of reactive nitrogen species, and the oxidation chemistry of a pollution plume are central to the goals of the TRACE-P mission. Although beyond the scope of this paper, the chemical evolution of this polluted layer has been investigated in detail using a 3-D model [*Heald et al.*, this issue] and Lagrangian trajectory modeling [*A. Hamlin*, in preparation].

It is expected that this polluted plume does not represent an isolated incident. It more likely represents an episodic transport pathway for emissions from the Asian Pacific Rim. The extent to which this particular transport pathway can be diagnosed from MOPITT observations is highlighted by this analysis. Given the additional details provided by the full suite of TRACE-P measurements, further attempts to diagnose the frequency and magnitude of similar transport events using MOPITT data would be useful not just for understanding CO. Some expectation of the impact on other species could be made by inference from the TRACE-P aircraft data.

7. Conclusion

Airborne sampling over the central North Pacific during TRACE-P revealed a polluted layer characterized by enhanced CO mixing ratios between 600-800 hPa that were more than double background values for the rest of the column. Sampling of this layer included a vertical profile conducted in coincidence with an overpass of the MOPITT instrument onboard the EOS Terra

1   satellite. This profile, along with sampling over the surrounding area by NASA's DC-8 and P-3B

2   aircraft revealed that the layer covered a geographic range of at least 25 degrees longitude (~2500

3   km) and 4 degrees latitude (~400 km).

4   The full geographic extent of the layer was estimated using back-trajectory analysis. The layer

5   then was tracked back in time to examine the overlap between the feature and MOPITT observations

6   for four consecutive overpasses. The MOPITT data for these four overpasses showed clear signs

7   of enhanced CO column associated with the position of the layer as diagnosed by trajectories.

8   Enhancements in MOPITT CO column and the trajectories agreed well. However, the average CO

9   column associated with the trajectories increased by 21 percent back in time across the 36 hours

10   covered by the four overpasses. Several possible reasons for the change in average CO column were

11   investigated. These included chemistry, dilution, change in the thickness of the layer, and the

12   sensitivity of the MOPITT retrieval to the altitude of the layer.

13   Results of this analysis suggest that most of the change in average CO column is consistent with

14   a physical change in the thickness of the layer (9 percent) and changes in the retrieved column

15   amount due to the altitude of the layer (7 percent). Changes due to chemistry were estimated to be

16   much smaller (2.5 percent), and the impact of dilution, while difficult to quantify, was expected to

17   be even smaller. Taken together, these impacts can account for 90 percent of the observed change

18   in MOPITT CO column.

19   An examination of the altitude of individual trajectories versus MOPITT CO column revealed

20   a good correlation (R^2=0.62) and a trend similar to that expected based on the sensitivity of the

21   MOPITT retrieval to the altitude of the layer. This exercise also revealed greater variability in CO

22   column for daytime versus nighttime observations. Currently, there is no clear explanation for this

23   behavior.

17

1   These results provide insight on the sources of variability (both real and artificial) in satellite

2   observations. They also suggest that validation strategies might benefit from broader regional

3   sampling in support of validation profiles as well as pre-planned targeting of large-scale features.

4   This also would facilitate the evaluation of forward-trajectories and global/regional models used to

5   forecast the presence and timing of pollution transport. The importance of the link between aircraft

6   and satellite data is demonstrated here in the wealth of detail that in situ observations provide

7   versus the long term tracking of transport through satellite observations. While the airborne data

8   provide the opportunity for a detailed examination of the chemical evolution of transport from the

9   Asian Pacific Rim to the central North Pacific, satellite observations from MOPITT offer the

10   possibility of monitoring the frequency and strength of such transport events.

1   **References:**

2   Bengtsson, L., Medium-range forecasting-The experience of ECMWF, *Bull. Am. Meteorol. Soc.*,

3   *66*, 1133-1146, 1985.

4   Deeter, M. N., G. L. Francis, D. P Edwards, J. C. Gille, E. McKernan, and J. R. Drummond,

5   Operational validation of the MOPITT instrument optical filters, *J. Atm. and Oceanic Tech.*, *19*,

6   1772-1782, 2002.

7   Deeter, M. N., et al., Operational carbon monoxide retrieval algorithm and selected results for the

8   MOPITT instrument, *J. Geophys. Res.*, *108*(D14) , 4399, doi:10.1029/2002JD003186, 2003.

9   Drummond, J. R., and G. S. Mand, The Measurements of Pollution in the Troposphere (MOPITT)

10   instrument: Overall performance and calibration requirements, *J. Atm. and Oceanic Tech.*, *13*,

11   314-320, 1996.

12   Eisele, F. L., et al., Summary of measurement intercomparisons during TRACE-P, *J. Geophys. Res.*,

13   *108*(D20), 8791, doi:10.1029/2002JD003167, 2003.

14   Emmons, L. K., et al., Validation of MOPITT CO retrievals with aircraft *in situ* profiles, *J. Geophys.*

15   *Res.*, submitted, 2003.

16   European Centre for Medium-Range Weather Forecasts (ECMWF), User guide to ECMWF products

17   2.1, *Meteorol. Bull. M3.2*, Reading England, U.K., 1995.

18   Fishman, J., C. E. Watson, J. C. Larsen, and J. A. Logan, Distribution of tropospheric ozone

19   determined from satellite data, *J. Geophys. Res.*, *95*, 3599-3617, 1990.

20   Fishman, J., J. M. Hoell Jr., R. D. Bendura, R. J. McNeal, V. W. J. H. Kirchoff, NASA GTE

21   TRACE A experiment (September-October 1992): Overview, *J. Geophys. Res.*, *101*, 23,865-

22   23,879, 1996.

23   Fuelberg H. E., R. O. Loring Jr., M. V. Watson, M. C. Sinha, K. E. Pickering, A. M. Thompson, G.

1   W Sachse, D. R. Blake, and M. R. Schoeberl, TRACE-A trajectory imtercomparison 2.

2   Isentropic and kinematic methods, *J. Geophys. Res.*, *101*, 23,927-23,939, 1996.

3   Fuelberg H. E., R. E. Newell, S. P Longmore, W. Zhu, D. J. Westberg, E. V. Browell, D. R. Blake,

4   G. L. Gregory, and G. W. Sachse, A meteorological overview of the PEM-Tropics period, *J.*

5   *Geophys. Res.*, *104*, 5585-5622, 1999.

6   Fuelberg H. E., J. R. Hannan, P. F. J. van Velthoven, E. V. Browell, G. Bieberbach Jr., R. D. Knabb,

7   G. L. Gregory, K. E. Pickering, and H. B. Selkirk, A meteorological overview of the SONEX

8   period, *J. Geophys. Res.*, *105*, 3633-3651, 2000.

9   Heald, C. L., et al., Transpacific satellite and aircraft observations of Asian pollution, *J. Geophys.*

10   *Res.*, this issue.

11   Hollingsworth, A., D. B. Shaw, P. Lonnberg, L. Illari, K. Arpe, and A. J. Simmons, Monitoring of

12   observations and analysis quality by a data assimilation system, *Mon. Weather Rev.*, *114*, 861-

13   879, 1986.

14   Jacob, D. J., J. H. Crawford, M. M. Kleb, V. S. Connors, R. J. Bendura, J. L. Raper, G. W. Sachse,

15   J. C. Gille, L. Emmons, and C. L. Heald, The Transport and Chemical Evolution over the Pacific

16   (TRACE-P) mission: Design, execution and overview of results, *J. Geophys. Res.*, *108*(D20),

17   8781, doi:10.1029/2002JD003276, 2003.

18   Maloney, J. C., H. E. Fuelberg, M. A. Avery, J. H. Crawford, D. R. Blake, B. G. Heikes, G. W.

19   Sachse, S. T. Sandholm, H. Singh, and R. W. Talbot, Chemical characteristics of air from

20   different source regions during the second Pacific Exploratory Mission in the Tropics (PEM-

21   Tropics B), *J. Geophys. Res.*, *106*, 32,609-32,625, 2001.

22   Novelli, P. C., K. A. Masarie, and P. M. Lang, Distributions and recent changes of carbon monoxide

23   in the lower trospospehre, *J. Geophys. Res.*, *103*, 19,015-19,033, 1998.

20

1   Sachse, G. W., G. F. Hill, L. O. Wade, and M. G. Perry, Fast-response, high-precision carbon

2   monoxide sensor using a tunable diode laser absorption technique, *J. Geophys. Res.*, *92*, 2071-

3   2081, 1987.

4   Singh, H. B. and D. J. Jacob, Future directions: Satellite observations of tropospheric chemistry,

5   *Atmos. Environ.*, *34*, 4399-4401, 2000.

6   Stohl, A., Computation, accuracy, and application of trajectories-A review and bibliography, *Atmos.*

7   *Environ.*, *32*, 947-966, 1998.

8   Vay, S. A., et al., DC-8-based observations of aircraft CO, CH_4, N_2O, and $H_2O_{(g)}$ emission indices

9   during SUCCESS, *Geophys. Res. Lett.*, *25*, 1717-1720, 1998.

1   **Figure Captions:**

2   **Figure 1.** a) Results from a MOPITT validation profile conducted by the NASA DC-8 on 27 Feb.,

3   2001. In situ data have been averaged to the MOPITT vertical resolution and processed using the

4   MOPITT averaging kernel to allow for direct comparison. b) Vertical distribution of CO data

5   collected on 27 Feb., 2001 from the NASA DC-8 and P-3 B aircraft. Data consists of 10 individual

6   soundings between 170E and 165W. c) Geographic distribution of samples between 600hPa and

7   800 hPa associated with the layer of enhanced CO mixing ratios and their proximity to the MOPITT

8   overpass

9

10   **Figure 2.** Transport history for an ensemble of trajectories with a common Asian Pacific Rim

11   origin. Trajectories were isolated from a larger set of back trajectories initialized at 700 hPa

12   between 10-25N and 162E-165W. These trajectories approximate the spatial extent of the polluted

13   layer which had been subsiding over the central, North Pacific for 3 days.

14

15   **Figure 3.** Overlap between the ensemble of trajectories and MOPITT for four consecutive

16   overpasses.

17

18   **Figure 4.** Calculated (crosses) and observed (circles) changes in MOPITT total CO column based

19   on changes in the vertical location of the polluted layer. The calculated changes represent

20   differences in retrieved column caused by moving the polluted layer upward and downward through

21   the troposphere in 100 hPa increments from 700 hPa where the layer was sampled. The observed

22   changes are based on the average MOPITT CO column and average pressure level of the trajectories

23   in the overlap region (see Table 1).

24

1 **Figure 5.** Same as Figure 4 except individual MOPITT observations are shown for each MOPITT

2 overpass instead of average conditions within the overlap. Vertical displacement of a given

3 MOPITT observation is based on the nearest trajectory.

4

5

6

1 Table 1. Statistics for MOPITT CO column and trajectories in the overlap region.

Overpass Date/Time	Average CO column in overlap (10^{18} molec cm^{-2})	Average pressure level of trajectories in overlap (hPa)	Average thickness of CO layer in overlap (hPa)[a]
27 Feb., 2231 UT	2.27 ± 0.18	700 ± 2	190 ± 4
27 Feb., 1021 UT	2.32 ± 0.10	685 ± 15	193 ± 32
26 Feb., 2148 UT	2.71 ± 0.30	628 ± 24	252 ± 44
26 Feb., 0938 UT	2.75 ± 0.15	588 ± 36	282 ± 33

7 a-based on the average difference between trajectories initiated at 800hPa and 615 hPa.

10 Table 2. MOPITT CO column statistics versus Cloud Flag

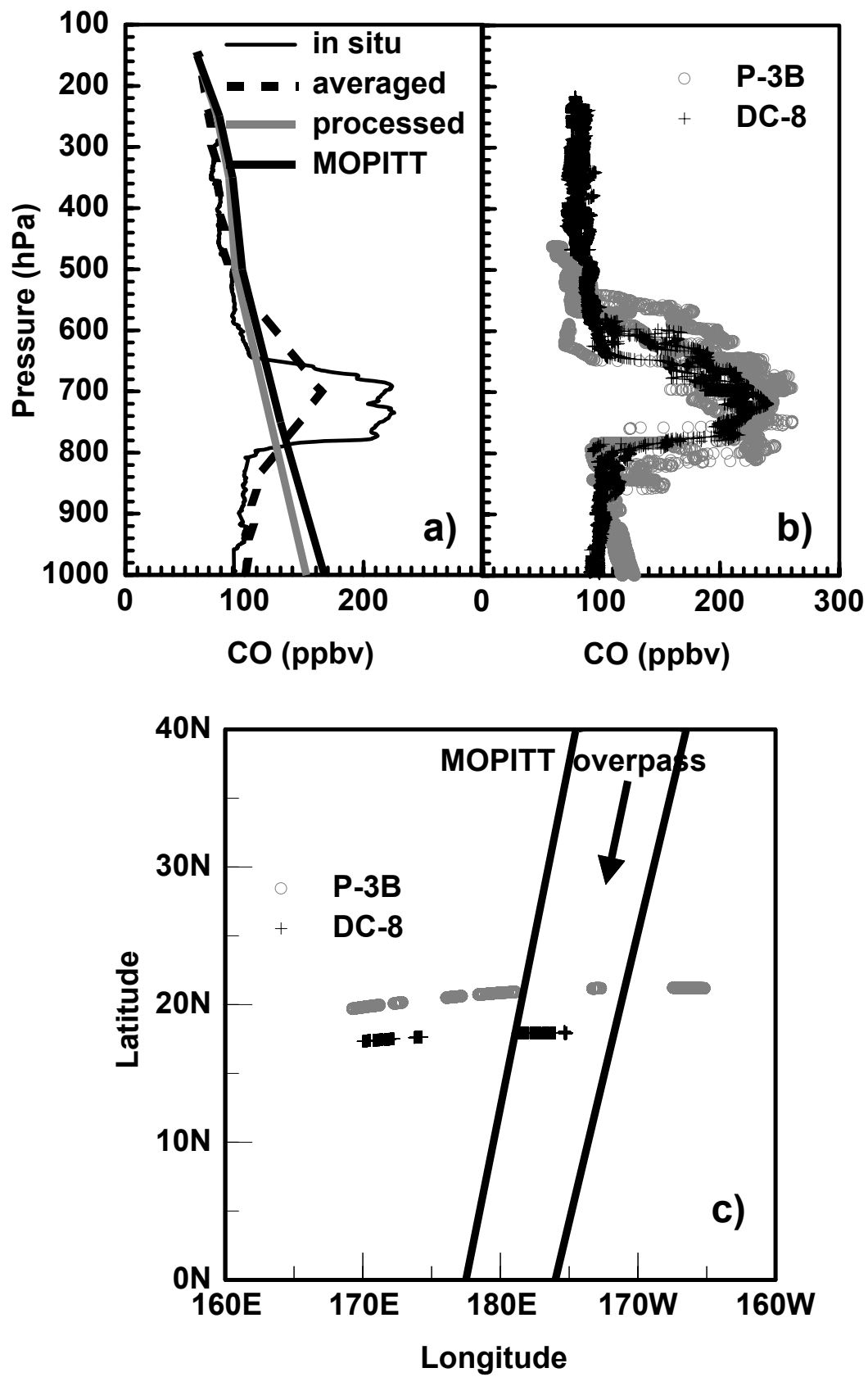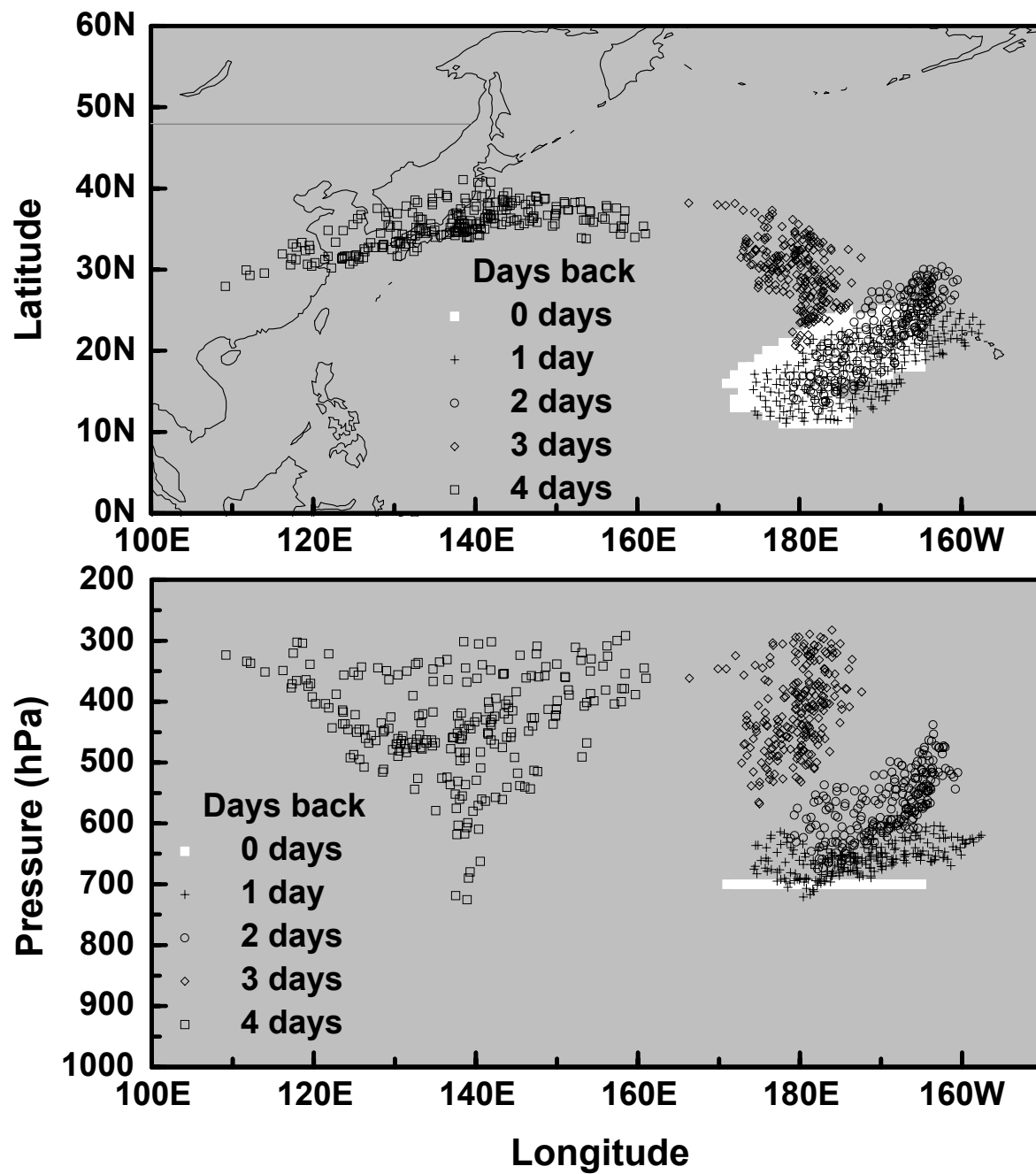|	Daylight Conditions		Dark Conditions	
	27 February, 2231 UT		27 February, 1021 UT	
Cloud Flag	% data	CO ± st. dev.	% data	CO ± st. dev.
1	1	2.41 ± 0.20	5	2.28 ± 0.11
2	40	2.27 ± 0.17	13	2.30 ± 0.10
3	3	2.16 ± 0.35	no data	no data
4	56	2.28 ± 0.17	82	2.32 ± 0.10
	26 February, 2148 UT		26 February, 0938 UT	
Cloud Flag	% data	CO ± st. dev.	% data	CO ± st. dev.
1	2	2.45 ± 0.28	20	2.66 ± 0.10
2	46	2.68 ± 0.28	6	2.66 ± 0.12
3	4	2.76 ± 0.39	1	2.65 ± 0.12
4	48	2.75 ± 0.30	73	2.78 ± 0.15

Figure 1

Figure 2

Figure 3

Figure 4

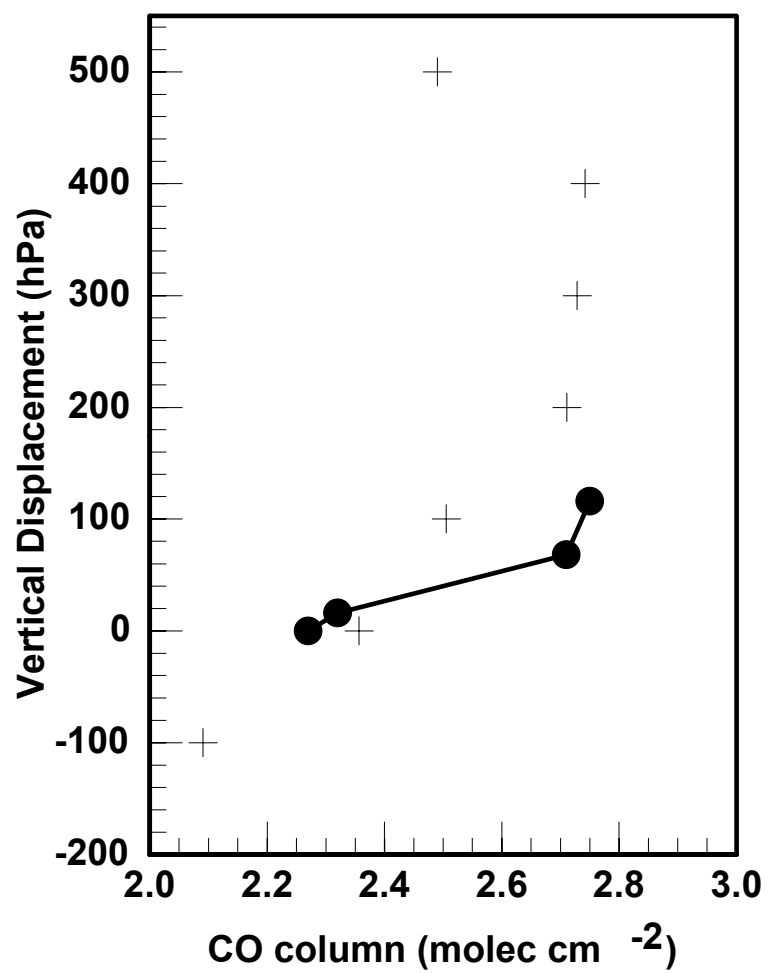# Figure 5